Malaysian Journal of Chemistry, 2020, Vol. 22(3), 100-110
(Special Issue: *International Conference in Organic Synthesis - ICOS 2019, Universiti Teknologi MARA*)

Anti-Amoebic Activity of Eugenol Derivatives against *Acanthamoeba castellanii*

Khairunisa Mohd Zamli[1], Asnuzilawati Asari[1,2*], Fatimah Hashim[1], Hanis Mohd Yusoff[1,2], Habsah Mohamad[3] and Fauziah Abdullah[4]

[1]Faculty of Science and Marine Environment, Universiti Malaysia Terengganu, 21030 Kuala Nerus, Terengganu, Malaysia
[2]Advanced Nano Materials (ANoMa) Research Group, Faculty of Science and Marine Environment, Universiti Malaysia Terengganu, 21030 Kuala Nerus, Terengganu, Malaysia
[3]Institute of Marine Biotechnology, Universiti Malaysia Terengganu, 21030 Kuala Nerus, Terengganu, Malaysia
[4]Natural Product Division Forest Research Institute of Malaysia, 52109 Kepong, Selangor, Malaysia
*Corresponding author (e-mail: asnu@umt.edu.my)

Eugenol is the major compound of clove and has demonstrated various pharmacological activities. In this study, nine eugenol derivatives (**1**-**9**) were synthesized, characterized, and further evaluated for their anti-amoebic properties against *Acanthamoeba castellanii (A. castellanii*) trophozoites. The derivatives were obtained through etherification or esterification reaction at the hydroxyl group (-OH) of eugenol. The chemical structures of the synthesized derivatives were characterized on the basis of ^{1}H and ^{13}C Nuclear Magnetic Resonance (NMR) spectroscopy and Fourier Transform Infrared (FTIR) spectroscopy. For anti-amoebic activity, the cytotoxicity of the derivatives was tested on *A. castellanii* trophozoites. The samples were prepared at varying concentrations (in the range of 0.47 to 60 μg/mL). The IC_{50} values were examined based on MTT assay while light and fluorescence microscopy were used to visualize the morphology changes of amoeba in detail. The results obtained were compared with the standard drug, which was chlorhexidine. Several of the tested derivatives possessed cytotoxic effects against throphozoite cells with IC_{50} in the range of 0.58 to 27.83 μg/mL with significant decrease ($p < 0.05$) in cell viability as the concentration was increased up to 30 μg/mL. Among them, derivative **4** provided the strongest cytotoxic effect against *A. castellanii*, suggesting a promising new anti-amoebic agent. Altogether, this finding may potentially serve as the milestone for developing an alternative treatment for *Acanthamoeba* keratitis.

Key words: Eugenol derivatives; trophozoite; *Acanthamoeba*; MTT assay

Received: December 2019; Accepted: May 2020

Acanthamoeba is a free-living protozoon that occupies most habitats in the environment [1]. It can be found commonly in soil, air, dust, and water collections, which include tap water, swimming pool, bottled water, and even contact lens solution [2,3]. The life cycle of *Acanthamoeba* consists of a vegetative trophozoite and a resistant cyst stage. *Acanthamoeba* can be maintained in trophozoite with food supply, appropriate temperature, and neutral pH. However, when the environmental conditions become unfavorable, it will induce the transformation of trophozoite into the cyst stage [4]. To date, several species of genus *Acanthamoeba* are known to cause the sight-threatening disease *Acanthamoeba* keratitis (AK) that affects mainly contact lens users. As of study in 2007, more than 3000 cases of AK were reported worldwide [5]. It is clear that the number of AK reported cases continues to increase due to the rising number of contact lens users in recent years.

Currently, an efficient medical treatment for treating this *Acanthamoeba*-caused infection is still not available. The existing drugs such as chlorhexidine and polyhexamethylene biguanide are employed to minimize the symptoms, not particularly designed to treat ocular disease, and thus often endowed with unpleasant side effects [6,7]. Moreover, the presence of *Acantamoeba* strains that are resistant to these drugs and the existence of the cyst phase make them less effective [8,9]. If AK is not diagnosed early, the corneal epithelium becomes ulcerated with stromal infiltration, leading to a perforation ring in filtrate and finally loss of vision [10]. This situation gives rise to the urgent need for the development of drugs as to overcome the

†Paper presented at the International Conference in Organic Synthesis (ICOS 2019), 9-10 December 2019, Universiti Teknologi MARA.

problem.

There is a growing interest in using natural products, especially essential oils, which are generally recognized as safe (GRAS) against bacteria of clinical origin, fungi, and viruses [11]. Many previously reported studies have shown that eugenol and its derivatives exhibited a wide spectrum of functional properties in pharmaceuticals, such as antiseptic [12], anticancer [13,14], anti-bacterial [15], and anti-inflammatory [16]. For example, Carassco *et al*. [13] claimed that eugenol derivatives, which were 5-allyl-3-nitrobenzene-1,2-diol and 2-methoxy-5-nitrophenyl acetate had shown potential human tumor cell growth inhibitory effects. Recently, a special attention was also given to their anti-amoebic activity. According to Anacarso *et al*. [17], eugenol showed a good anti-amoebic activity which could represent a promising alternative to treat infectious diseases which concern *Acanthamoeba*-caused infections. But, the potential anti-amoebic activity of eugenol derivatives remains limitedly explored. Therefore, in this study, eugenol was subjected to etherification or esterification reaction to obtain the stable desired molecules. Then, they were further subjected to cytotoxicity test against *Acanthamoeba castellanii* (*A. castellanii*) which involved the inhibition analysis of amoeba population. Microscopic observations were also implemented to examine the disruption of the amoeba membrane integrity and morphological changes in the amoeba cells caused by these synthesized compounds.

MATERIALS AND METHODS

1. Chemistry

All chemicals and reagents utilized in this study were obtained from Merck, Sigma-Aldrich, Acros Organics, and R&M with no further purification. Briefly, all reactions were carried out under nitrogen atmosphere. Thin-layer chromatography (TLC) on silica gel plates coated with fluorescence indicator F254 (Merck, Germany) was used to monitor the reaction course. Column chromatography was performed on silica gel 60 (0.040-0.063 mm, 230-400 mesh, Merck). All purified compounds were structurally elucidated, mainly via Nuclear Magnetic Resonance (NMR) spectra on Bruker FT-400 Spectrophotometer by using chloroform ($CDCl_3$) as solvent. Chemical shifts are expressed as ppm values for both ^1H and ^{13}C=NMR. Infrared spectra were recorded on Shimadzu IRTracer-100 Fourier Transform Infrared Spectrometer (FTIR) that ranged from 400 to 4000 cm^{-1} by using single reflection ATR.

2. Synthesis of Eugenol Derivative (1)

The etherification reaction was carried out as a previously reported method [18] with slight modifications. To a solution of eugenol (1 eq) in anhydrous acetone (20 mL), potassium carbonate (1 eq) and alkyl halide (1.5 eq) were added. The reaction mixture was refluxed under an inert condition for a period of 24 h. The complete disappearance of the starting material was confirmed by TLC. Afterward, the reaction mixture was diluted with distilled water (20 mL) and then extracted with dichloromethane (3 × 20 mL). The organic layer was filtered, dried with $MgSO_4$ and concentrated under reduced pressure so as to remove the residual solvent. The pure product was obtained by column chromatography (silica gel, hexane-ethyl acetate), which gave the desired derivative 1 at 77% yield.

2.1. 4-Allyl-2-methoxy-1-(4-trifluoromethyl-benzyloxy)-benzene (1)

Yield: 77%; ATR 3012, 2935, 1643, 1512, 1230, 1107, 1064 cm^{-1}; ^1H-NMR (400 MHz, $CDCl_3$) δ 3.24 (d, J 6.4 Hz, 2H, CH_2), 3.80 (s, 3H, OCH_3), 4.96-5.02 (m, 2H, CH_2), 5.09 (s, 2H, CH_2), 5.81-5.92 (m, 1H, CH), 6.57-6.59 (dd, J 8.0 Hz, J 2.0 Hz, 1H, CH_{ar}), 6.66 (d, J 2.0 Hz, 1H, CH_{ar}), 6.68 (d, J 8.0 Hz, 1H, CH_{ar}), 7.46 (d, J 8.4 Hz, 2H, CH_{ar}), 7.52 (d, J 8.4 Hz, 2H, CH_{ar}) ppm; ^{13}C-NMR (100 MHz, $CDCl_3$) δ 39.8, 55.9, 70.4, 112.4, 114.3, 115.7, 120.4, 122.8, 125.5, 127.2, 129.7, 133.8, 137.5, 141.5, 146.1, 149.6 ppm.

3. Synthesis of Eugenol Derivatives (2-9)

Derivatives **2-9** were synthesized by following a previously published method [18] with slight modifications. Anhydrous dichloromethane (20 mL) was added in a solution of eugenol (1 eq), followed by the addition of trimethylamine (2.5 mL). The reaction mixture was stirred for 30 min at 0-5°C under nitrogen flow. Thereafter, an excess of acyl chloride (2 eq) was added dropwise within 15 min. The mixture was stirred for another 30 min at 0-5°C and left to continue stirring at room temperature for another 24 h. The completion of reaction was confirmed by TLC. Then, the reaction mixture was diluted with distilled water and extracted with dichloromethane (3 × 20 mL). The combined organic layer was dried over $MgSO_4$. After the solvent was removed in vacuo, the residue was purified by column chromatography using silica gel with hexane/ethyl acetate (3:1). The collected product after separation was dried under atmospheric pressure to obtain the desired derivatives (**2-9**) at 77 to 92% yields.

3.1. 4-Allyl-2-methoxyphenyl-4-ethylbenzoate (2) [41]

Yield: 92%; ATR 3012, 2974, 1724, 1604, 1504, 1261, 1029 cm^{-1}; ^1H-NMR (400 MHz,$CDCl_3$) δ 1.29-1.33 (t, *J* 7.6 Hz, 3H, CH_3), 2.74-2.80 (q, *J* 7.6 Hz, 2H, CH_2), 3.43 (d, *J* 6.4 Hz, 2H, CH_2), 3.82 (s, 3H, OCH_3), 5.12-5.18 (m, 2H, CH_2), 5.96-6.07 (m, 1H, CH), 6.82-6.85 (dd, *J* 8.0 Hz,*J* 2.0 Hz, 1H, CH_{ar}), 6.86 (d, *J* 1.6 Hz, 1H, CH_{ar}),

Table 1. The molecular structures of the eugenol-derived molecules

Code	IUPAC name	Molecular structure
1	4-Allyl-2-methoxy-1-(4-trifluoromethyl-benzyloxy)-benzene	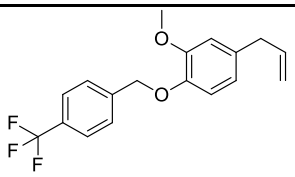
2	4-Allyl-2-methoxyphenyl-4-ethylbenzoate	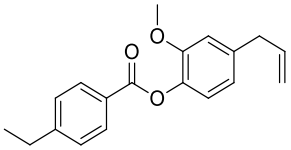
3	4-Allyl-2-methoxyphenyl-4-nitrobenzoate	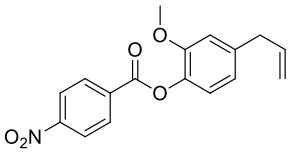
4	4-Allyl-2-methoxyphenyl-4-methoxybenzoate	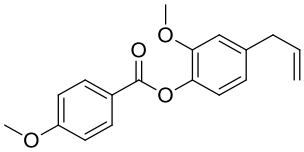
5	4-Allyl-2-methoxyphenyl-4-bromobenzoate	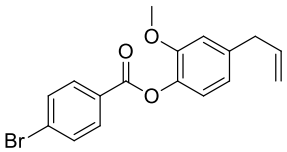
6	4-Allyl-2-methoxyphenyl-4-fluorobenzoate	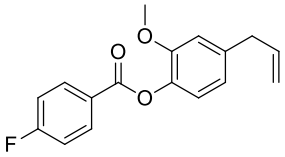
7	4-Allyl-2-methoxyphenyl-3-bromobenzoate	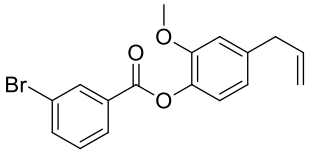
8	4-allyl-2-methoxyphenyl-4-(tert-butyl)benzoate	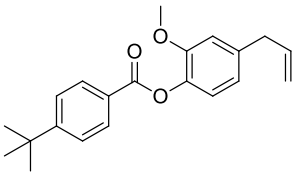
9	4-allyl-2-methoxyphenyl-4-(trifluoromethyl) benzoate	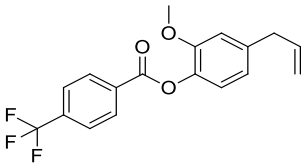

7.08 (d, *J* 8.0 Hz, 1H, CH_{ar}), 7.34 (d, *J* 8.4 Hz, 2H, CH_{ar}), 8.15 (d, *J* 8.4 Hz, 2H, CH_{ar}) ppm; ^{13}C-NMR (100 MHz, $CDCl_3$) δ 15.3, 29.0, 40.1, 55.9, 112.8, 116.1, 120.7, 122.7, 126.9, 128.0. 130.4, 137.1, 138.2, 138.9, 150.3, 151.1, 164.9 ppm.

3.2. 4-Allyl-2-methoxyphenyl-4-nitrobenzoate (3) [20]

Yield: 87%; ATR 3005, 2939, 1743, 1600, 1527, 1504, 1342, 1265, 1072 cm^{-1}; ^{1}H-NMR (400 MHz, $CDCl_3$) δ 3.43 (d, *J* 6.8 Hz, 2H, CH_2), 3.83 (s, 3H, OCH_3), 5.12-5.18 (m, 2H, CH_2), 5.96-6.06 (m, 1H, CH), 6.84-6.87 (dd, *J* 8.0 Hz, *J* 2.0 Hz, 1H, CH_{ar}), 6.87 (d, *J* 1.6 Hz, 1H, CH_{ar}), 7.09 (d, *J* 8.0 Hz, 1H, CH_{ar}), 8.35-8.42 (m, 4H, CH_{ar}) ppm; ^{13}C-NMR (100 MHz, $CDCl_3$) δ 40.1, 55.8, 112.8, 116.3, 120.8, 122.3, 123.6, 131.4, 134.9, 136.9, 137.7, 139.6, 150.7, 150.8, 163.0 ppm.

3.3. 4-Allyl-2-methoxyphenyl-4-methoxybenzoate (4) [15]

Yield: 77%; ATR 3012, 2943, 1724, 1604, 1508, 1261, 1026 cm^{-1}; ^{1}H-NMR (400 MHz, $CDCl_3$) δ 3.42 (d, *J* 6.8 Hz, 2H, CH_2), 3.82 (s, 3H, OCH_3), 3.91 (s, 3H, OCH_3),), 5.11-5.18 (m, 2H, CH_2), 5.96-6.06 (m, 1H, CH), 6.82-6.84 (dd, *J* 8.0 Hz, *J* 2.0 Hz, 1H, CH_{ar}), 6.85 (d, *J* 1.6 Hz, 1H, CH_{ar}), 6.99 (d, *J 8*.8 Hz, 1H, CH_{ar}), 7.07 (d, *J* 8.0 Hz, 2H, CH_{ar}), 8.18 (d, *J* 9.2 Hz, 2H, CH_{ar}) ppm; ^{13}C-NMR (100 MHz, $CDCl_3$) δ 40.1, 55.5, 55.9, 112.8, 113.7, 116.1, 120.7, 121.8, 122.7, 132.4, 137.1, 138.3, 138.9, 151.2, 163.7, 164.6 ppm.

3.4. 4-Allyl-2-methoxyphenyl-4-bromobenzoate (5) [18]

Yield: 89%; ATR 3008, 2935, 1735, 1639, 1504, 1261, 1064, 1029 cm^{-1}; ^{1}H-NMR (400 MHz, $CDCl_3$) δ 3.43 (d, *J* 6.8 Hz, 2H, CH_2), 3.82 (s, 3H, OCH_3), 5.12-5.19 (m, 2H, CH_2), 5.96-6.06 (m, 1H, CH), 6.83-6.85 (dd, 8.0 Hz, 2.0 Hz, 1H, CH_{ar}), 6.86 (d, *J* 1.2 Hz, 1H, CH_{ar}), 7.08 (d, *J* 8.0 Hz, 1H, CH_{ar}), 7.65 (d, *J* 8.4 Hz, 2H, CH_{ar}), 8.09 (d, *J* 8.8 Hz, 2H, CH_{ar}) ppm; ^{13}C-NMR (100 MHz, $CDCl_3$) δ 40.1, 55.8, 112.8, 116.2, 120.7, 122.5, 128.4, 128.6, 131.1, 131.7, 137.06, 138.0, 139.2, 151.0, 164.1 ppm.

3.5. 4-Allyl-2-methoxyphenyl-4-fluorobenzoate (6) [21]

Yield: 78%; ATR 3020, 2985, 1732, 1600, 1508, 1265, 1203, 1149, 1068 cm^{-1}; ^{1}H-NMR (400 MHz, $CDCl_3$) δ 3.43 (d, *J* 6.4 Hz, 2H, CH_2), 3.83 (s, 3H, OCH_3), 5.12-5.18 (m, Hz, 2H, CH_2), 5.98-6.06 (m, 1H, CH), 6.83-6.85 (dd, *J* 8.0 Hz,*J*2.0 Hz, 1H, CH_{ar}), 6.86 (d, *J* 1.6 Hz, 1H, CH_{ar}), 7.07 (d, *J* 8.0 Hz, 1H, CH_{ar}), 7.17 (t, *J* 8.8 Hz, 2H, CH_{ar}), 8.24-8.27 (dd *J* 8.8 Hz,*J*5.2 Hz, 2H, CH_{ar}) ppm; ^{13}C-NMR (100 MHz, $CDCl_3$) δ 40.1, 55.8, 112.8, 115.8, 116.2, 120.7, 122.6, 125.7, 132.8, 137.0, 138.0, 139.1, 151.0, 163.9, 164.8, 167.3 ppm.

3.6. 4-Allyl-2-methoxyphenyl-3-bromobenzoate (7)

Yield: 81%; ATR3070, 2962, 1735, 1639, 1504, 1246, 1072, 1033 cm^{-1}; ^{1}H-NMR (400 MHz, $CDCl_3$) δ 3.43 (d, *J* 6.8 Hz, 2H), 3.83 (S, 3H, OCH_3), 5.12-5.18 (m, 2H, CH_2), 5.96-6.06 (m, 1H, H2), 6.83-6.85 (dd, *J* 8.0 Hz,*J* 2.0 Hz, 1H, CH_{ar}), 6.86 (d, *J* 1.6 Hz, 1H, CH_{ar}), 7.07 (d, *J* 7.6 Hz, 1H, CH_{ar}), 7.39 (t, *J* 8.0 Hz, H, CH_{ar}), 7.76-7.79 (ddd, *J* 8.0 Hz,*J* 2.0 Hz, *J* 1.2 Hz, H, CH_{ar}), 8.15-8.17 (dt, *J* 7.6 Hz,*J* 1.2 Hz, H, CH_{ar}), 8.37 (t, *J* 2.0 Hz, H, CH_{ar}) ppm; ^{13}C-NMR (100 MHz, $CDCl_3$) δ 40.1, 55.8, 112.8, 116.2, 120.7, 122.5, 128.8, 130.0, 131.4, 133.2, 136.3, 137.0, 137.9, 139.3, 150.9, 163.5 ppm.

3.7. 4-allyl-2-methoxyphenyl 4-(tert-butyl) ben zoate (8)

Yield: 83%; ATR2962, 2908, 1732, 1639, 1508, 1269, 1064 cm^{-1}; ^{1}H-NMR (400 MHz, $CDCl_3$) δ 1.32 (s, 9H, $C(CH_3)_3$) 3.41 (d, *J* 6.8 Hz, 2H, CH_2), 3.73 (s, 3H, OCH_3), 5.07-5.16 (m, 2H, CH_2), 5.97-6.04 (m, 1H, H2), 6.80-6.83 (dd, *J* 8.4 Hz, *J* 2.0 Hz, 1H, CH_{ar}), 6.9 (d, *J* 1.6 Hz, 1H, CH_{ar}), 7.10 (d, *J* 8.0 Hz, 1H, CH_{ar}), 7.64 (d, *J* 8.8 Hz, 2H, CH_{ar}), 8.02 (d, *J* 8.0 Hz, 2H, CH_{ar}) ppm; ^{13}C-NMR (100 MHz, $CDCl_3$) δ 30.2, 34.3, 38.9, 55.0, 112.3, 115.4, 119.7, 122.1, 125.2, 125.6, 129.1, 129.7, 136.8, 138.3, 150.14, 156.5, 157.8, 161.8, 163.42 ppm.

3.8. 4-allyl-2-methoxyphenyl 4-(trifluoromethyl) benzoate (9)

Yield: 88%; ATR3008, 2939, 1739, 1639, 1508, 1265, 1134, 1072 cm^{-1}; ^{1}H-NMR (400 MHz) δ 3.43 (d, *J* 6.8 Hz, 2H, CH_2), 3.83 (s, 3H, OCH_3, H7), 5.13-5.19 (m, 1H, CH_2, H1), 5.96-6.06 (m, 1H, H2), 6.84-6.87 (dd, *J* 8.0 Hz,*J* 2.0 Hz, 1H, CH_{ar}), 6.878 (d, *J* 2.0 Hz, 1H, CH_{ar}), 7.09 (d, *J* 8.0 Hz, 1H, CH_{ar}), 7.78 (d, *J* 8.0 Hz, 2H, CH_{ar}), 8.34 (d, *J* 8.4 Hz, 2H, CH_{ar}) ppm; ^{13}C-NMR (100 MHz, $CDCl_3$) δ 40.1, 55.8, 112.8, 116.2, 120.7, 122.4, 125.5, 130.7, 132.7, 134.6, 135.0, 137.0, 137.9, 139.4, 150.9, 161.7 ppm.

4. Biological Activity

4.1. Protease yeast glucose (PYG) medium preparation

Protease yeast glucose (PYG) medium was prepared by mixing 3.75 g of protease, 3.75 g of yeast extract, and 7.5 g of D^+ glucose in 5 mL of Page's amoeba saline (PAS) solution. Distilled water was added until the volume was marked at 500 mL. Then, the medium was autoclaved and stored at 4°C prior to use.

4.2. Cell culture and maintenance

An *Acanthamoeba* sp. namely *A. castellanii* (HKL

isolate) was cultured in a T-25 tissue culture flask which contained 10 mL of PYG medium. The flask was kept in an incubator at 30°C and the medium changing process was done routinely to maintain healthy cell cultures. The condition of the cells was examined for any signs of contamination under an inverted microscope.

4.3. Sample stock solution

Stock solutions of the eugenol derivatives were prepared by dissolving 1 mg of each derivative in 40 µl of absolute DMSO, followed by adding 960 µL of sterile PYG medium to make a 1 mg/mL solution. Dissolution was facilitated by vortex and kept at 4°C before use. Seven different concentrations of the samples were prepared from the stock solutions through serial dilution to give the following final concentrations of the compounds: 30, 15, 7.50, 3.75, 1.88, 0.94 and 0.47 µg/mL. The concentration of DMSO in the most concentrated sample in treatment wells was 0.04% (w/v) and did not exceed 0.25% (w/v), which is the recommended threshold value of DMSO for anti-amoebic treatment [19]. Negative influences against studied amoeba will occur if the concentration of DMSO exceeds this value.

4.4. Determination of IC_{50} values by MTT assay

Experiments were carried out in a 96-well plate at 30°C under sterile conditions. Each well was seeded with a trophozoite suspension in triplicate (1×10^5 cells/well). After 24 h, the medium was removed after the cells were left to adhere to the bottom of the wells. Stock solutions of the eugenol derivatives at concentrations that ranged from 0.47 to 30 µg/mL was added to the treatment and incubated for another 24 h. Then, the medium was removed and wells were washed with phosphate-buffered saline (PBS) as to discard the remaining suspension. Next, 20 µl of 3-(4,5-dimethylthiazol-2-yl)-2,5-diphenyltetrazolium bromide (MTT) solution (5 mg/mL) in PBS was added to the each well and further incubated. After 4 h, 150 µl of DMSO was placed into the wells to dissolve the formed formazon crystal. The final solutions from all wells were read for their absorbance at 570 nm by ELISA microplate reader. The readings obtained were plotted in GraphPad Prism software version 8.0.1 (GraphPad Inc.) to get a nonlinear sigmoidal dose-response curve. The cytotoxic activity was expressed as the IC_{50} value that corresponded to the concentration of the compounds which inhibited 50% of the *Acanthamoeba* population. The *t*-test was performed, and $p < 0.005$ was considered as statistically significant.

4.5. Observation of *Acanthamoeba* morphology changes

Acanthamoeba (10^4 cells/mL) was treated with the eugenol derivatives at their IC_{50} concentration in 6-well plates at 30°C. After being incubated for 24 h, the morphological changes of *Acanthamoeba* were evaluated and compared with that observed in control cultures. The negative control was healthy *Acanthamoeba* without any treatment while the positive control was chlorhexidine, a common agent used for treating AK infection. Observations were made directly from the culture plates under an inverted microscope (Leica Leitz, Wetzlar, Germany), which can view the change on the acanthapodia structure as well as the shape and size of cells.

4.6. Evaluation of *Acanthamoeba* membrane integrity

Acridine orange (AO) and propidium iodide (PI) were used as fluorescence dyes to observe the integrity of *Acanthamoeba* membrane after the cells (10^4 cells/mL) were treated with the compounds at their IC_{50} concentrations. The treatments, including controls, were carried out in 6-well plates at 30°C for 24 h of incubation time. Then, the medium was removed and wells were washed with PBS before undergoing a further AO/PI staining process. A stock solution for AO/PI was prepared by adding 2 µl of AO (1 mg/mL) and 2 µl of PI (1 mg/mL) in 996 µl of PBS, following a previously reported technique [1]. The cell suspensions were then subjected to incubation for 15 min in the dark because the dyes were light sensitive. Later, the *Acanthamoeba* cell suspensions were observed directly under an inverted fluorescence microscope (Leica Dmire, Wetzlar, Germany) in the dark.

RESULTS AND DISCUSSION

1. Chemistry

In this study, nine eugenol derivatives (**Table 1**) were synthesized as described in **Scheme 1** by etherification or esterification reaction. The synthesis involved treatment of eugenol with variety of acyl or alkyl halide. The combination of eugenol with these acyl moieties is believed to have the ability to improve biological activities [20,21]. Differences in size and nature of the carbon chain substitutions can cause stereo-electronic variations that help to identify characteristics needed to enhance the activity performance of these molecules [22]. The main goal of analog synthesis is to maintain or improve the biological activities while removing unnecessary molecular complexity [23].

2. IC_{50} Values by MTT Assay

In the first part of the anti-amoebic activity, nine derivatives (**1-9**) were evaluated for their cytotoxicity properties on *A. castellanii* trophozoites. The results indicated that only several of the tested derivatives possessed cytotoxic effect with IC_{50} values that ranged from 0.58 to 27.83 µg/mL (**Table 2**).

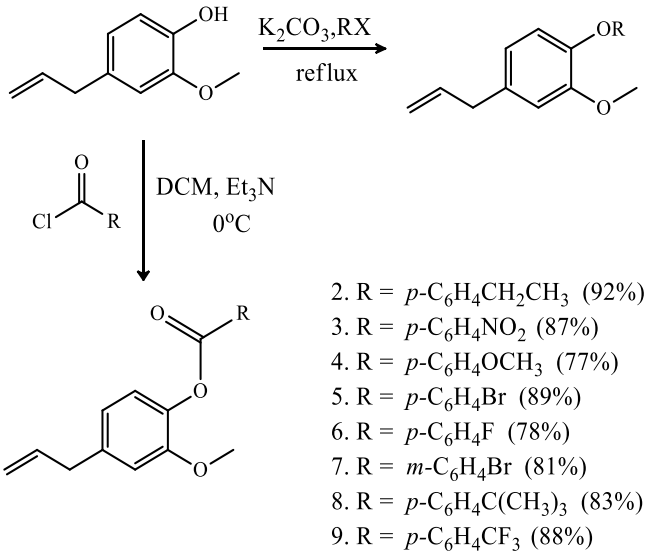

1. R = *p*-$C_6H_4CF_3$ (77%)
2. R = *p*-$C_6H_4CH_2CH_3$ (92%)
3. R = *p*-$C_6H_4NO_2$ (87%)
4. R = *p*-$C_6H_4OCH_3$ (77%)
5. R = *p*-C_6H_4Br (89%)
6. R = *p*-C_6H_4F (78%)
7. R = *m*-C_6H_4Br (81%)
8. R = *p*-$C_6H_4C(CH_3)_3$ (83%)
9. R = *p*-$C_6H_4CF_3$ (88%)

Scheme 1. Syntheses of eugenol derivatives through etherification or esterification reaction

Table 2. The IC_{50} values of eugenol derivatives against *A. castellanii*

Compound	IC_{50} (µg/mL)
1	7.53± 0.16
2	17.51± 0.15
3	-
4	0.58 ± 0.26
5	25.79± 0.13
6	-
7	-
8	27.83± 0.15
9	14.53 ± 0.16

-: not active up to conc. 30 µg/mL. The values are expressed as mean ± S.E.M from triplicate. (*t*-test, $p < 0.005$). Reference drug: Chlorhexidine (IC_{50}: 1.52 ± 0.45 µg/mL)

The results were statistically evaluated via analysis of variance by using *t*-test. The outcome data revealed significant differences ($p < 0.005$) between treated and untreated cells. Among them, derivative **4** which contained the methoxy substituent attached to the phenyl ring was found to be the most active derivative with IC_{50} of 0.58 µg/mL. A previous study by Bhutani *et al*. [24] concluded that methoxy substituent group in compounds would enhance the anti-amoebic activity.

With the same treatment duration, derivative **1** demonstrated a promising activity with IC_{50} of 7.53 µg/mL while derivative **9** demonstrated a moderate activity with IC_{50} of 14.53 µg/mL. Both derivatives bear a fluorine substituent at para position of the benzene ring. Derivative **5** also displayed a moderate toxicity with IC_{50} of 25.79 µg/mL. As emphasized by Gessler *et al*. [28], compounds with IC_{50} values of 10 to 50 µg/mL are classified as moderate toxicity while above 50 µg/mL are considered as non-toxic. For derivative **5**, it is believed that the presence of bromo substituent on the phenyl ring was responsible for the toxic properties on amoeba cells, which was similar to the finding by Abid and Azam [29].

Derivatives **2** and **8** demonstrated toxicity effect against *Acanthamoeba* with IC_{50} of 17.51 µg/mL and 27.83 µg/mL, respectively. Both derivatives contained an alkyl chain substituent attached to the phenyl ring. These results suggested that hydrophobicity of derivatives explained their action on *Acanthamoeba*. This finding was also supported by Boyam *et al*. [25], whereby hydrophobicity is an important feature that could improve the targeting of active components within compounds to intracellular protozoan parasites. Moreover, Bhutani *et al*. [24] also reported that electron donating groups on the aromatic part of the compounds have a vital role to increase the efficiency of these in vitro activities. The difference in IC_{50} values between derivatives **2** and **8** could be due to the difference in total

carbon substituents attached on the targeted parent compound. Variation length or total carbon group on compounds may also affect the amoebicidal activity [26]. According to Khairul *et al*. [27], compounds with higher molecular weights cause difficulty for the compounds to pass through the cell membrane.

3. *Acanthamoeba* Morphological Changes

Observations under light microscopy which showed the morphological structures of untreated and treated *Acanthamoeba* are shown in **Figures 1** and **2**. Untreated *Acanthamoeba* (normal trophozoites) illustrated the presence of thorn-like acanthapodia structure with prominent nuclei (**Figure 1a**). The cell cytoplasm was finely granular which held various ribosomes, mitochondria, food vacuoles, and a contractile vacuole. Acanthapodia possess an important feature in adhesion to surfaces, cellular movements, and capturing prey [30]. Throughout the trophozoite stage, amoeba feed on bacteria, algae and, yeast in the environment.

Meanwhile, derivative-treated *Acanthamoeba* showed loss of their acanthapodia structure and absence of vacuoles and nucli (**Figure 2**). The cells were observed to be rounded and floating in the culture

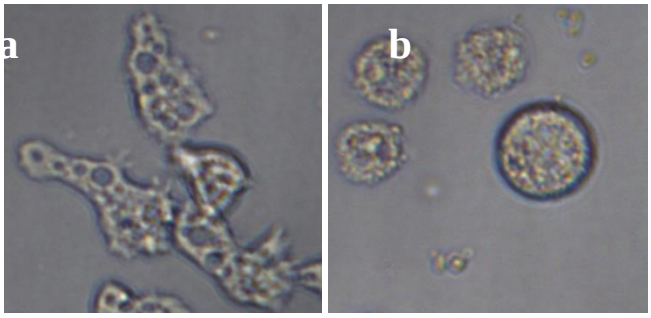

Figure 1. Light microscopy of *A. castellanii*:
(**a**) untreated amoeba; (**b**) chlorhexidine-treated amoeba. (magnification 600×)

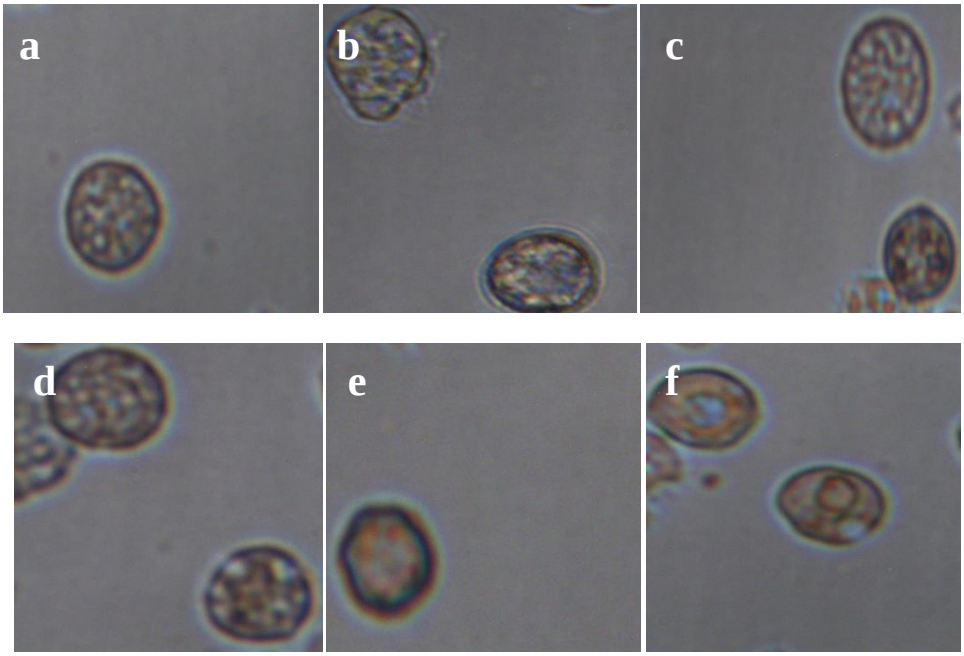

Figure 2. Light microscopy of *A. castellanii*: (**a**) **1**-treated amoeba; (**b**) **2**-treated amoeba;
(**c**) **4**-treated amoeba; (**d**) **5**-treated amoeba; (**e**) **8**-treated amoeba; (**f**) **9**-treated amoeba (magnification 600×)

medium as they were detached from the surface of the plate. The cells shrink caused the cytoplasm to become dense and the organelles were more tightly packed [31]. These transformations suggested that the cells had undertaken encystment process in response to environmental stress conditions [32]. In the present study, the morphological changes that were triggered by compounds could be signs of significant effects on the amoebicidal activity. Chlorhexidine-treated *Acanthamoeba* (**Figure 1b**) gave similar morphology changes as shown by the eugenol derivatives. The amoeba became circular and lost most of its water. The destruction of acanthapodia may lead to cell damage.

4. *Acanthamoeba* Membrane Integrity

In this study, AO and PI dual staining method was applied as to identify the integrity of the cells' membrane after being incubated with active compounds at their IC_{50} values as shown in **Figure 3**. Membrane integrity is crucial for cell survival. It is the feature most frequently used to identify whether cells are viable or non-viable. Cells which have lost membrane integrity can be classified as non-viable or dead [33]. Detection of non-viable cells is achieved by distinguishing the cells with compromised membrane from those of intact membrane [34]. Green to orange cytoplasm with orange stained lysosomes indicates a compromised cell membrane, while green cytoplasm with bright green lysosomes indicates an intact cell membrane [35]. According to Lovecka *et al.* [36], cytotoxic compounds can cause compromised cell membrane integrity.

Based on the results obtained, untreated *Acanthamoeba* or the negative control displayed round green stained cells (**Figure 3a**). They were indicated as viable cells with intact plasma membranes that only allowed the diffusion of AO. AO is a membrane-permeable dye which binds to DNA in healthy cells either by intercalating inside the double helix structure or electrostatic binding of the stack outside the double helix [37]. On the contrary, *Acanthamoeba* treated with chlorhexidine (positive control) as shown in **Figure 3b** revealed compromised membranes by displaying orange stained cells, indicating a total leakage of the cell membrane which allowed molecules to leak into the surrounding culture medium. An orange color will be emitted from cells under fluorescence microscopy because of stronger action of PI than AO [38]. PI is an impermeable dye, prohibited from entering healthy cells. It is only competent of binding to DNA upon the loss of membrane integrity and dead cells [39]. In short, PI could be used to differentiate between dead cells from living cells.

Meanwhile, *Acanthamoeba* treated with the given derivatives also showed compromised membranes, allowing PI dye to infiltrate into the cells and stain the lysosomes with orange color (**Figure 4**). The cells displayed nuclear fragmentation and cytoplasmic condensation because the membranes were damaged although the cells were colored green, the same as viable cells [40]. As a result, the active synthesized derivatives in the present study were proven to disrupt the plasma membrane integrity.

CONCLUSION

In conclusion, the amoebicidal activity of eugenol derivatives (**1**-**9**) against *A. castellanii* was successfully investigated. The results indicated that some of the derivatives have promising amoebicidal activities with IC_{50} that ranged from 0.58 to 27.83 μg/mL. Derivative **4** possessed the strongest toxicity properties as compared to the other tested compounds. Light microscopy study revealed that *Acanthamoeba* treated with derivatives at their IC_{50} values had lost their spine-like acanthapodia structure. Their membrane integrity was also proven to be disrupted under the fluorescence microscopy after being stained with AO/PI. Therefore, these derivatives can be presented as promising agents to treat *Acanthamoeba*-caused infections.

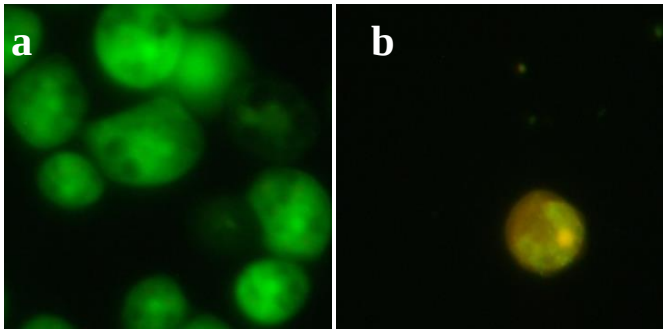

Figure 3. Fluorescence microscopy of *A. castellanii*:
(**a**) untreated amoeba; (**b**) chlorhexidine-treated amoeba. (magnification 600×)

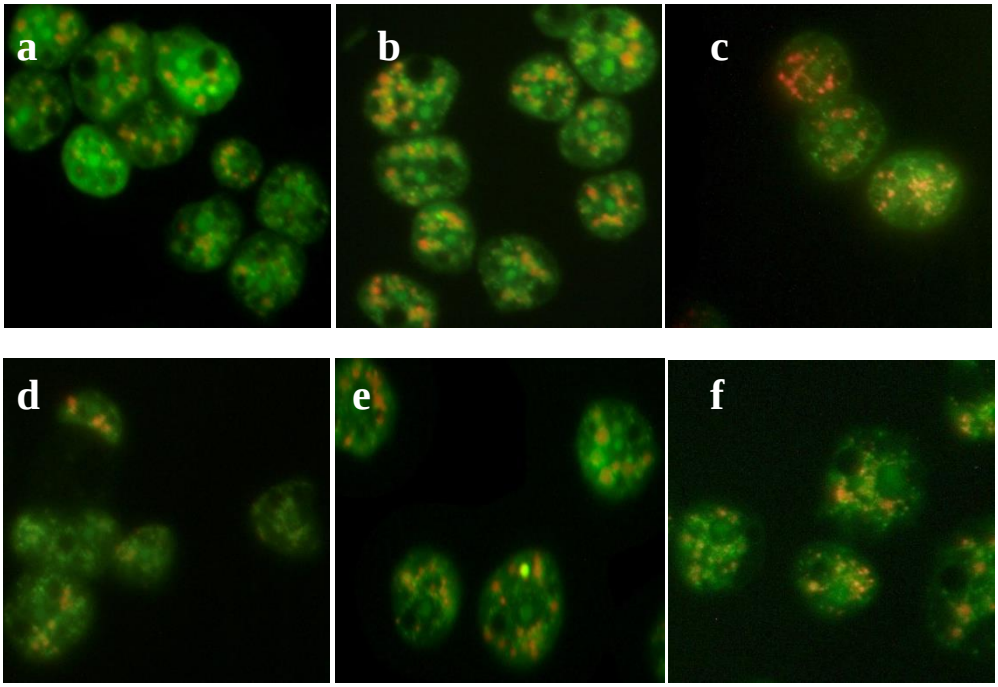

Figure 4. Fluorescence microscopy of *A. castellanii*: (**a**) **1**-treated amoeba; (**b**) **2**-treated amoeba; (**c**) **4**-treated amoeba; (**d**) **5**-treated amoeba; (**e**) **8**-treated amoeba;(**f**) **9**-treated amoeba (magnification 600×)

ACKNOWLEDGEMENT

The authors would like to thank the Faculty of Science and Marine Environment (FSSM), and The Institute of Oceanography (INOS), Universiti Malaysia Terengganu for providing the facilities to carry out this study.

REFERENCES

1. Nakisah, M. A., Muryany, M. I., Fatimah, H., Fadilah, R. N., Zalilawati, M. R., Khamsah, S. and Habsah, M. (2012) Anti-amoebic properties of a Malaysian marine sponge Aaptos sp. on Acanthamoeba castellanii. *World Journal of Microbiology and Biotechnology*, **28(3)**, 1237–1244.

2. Schuster, F. L. and Visvesvara, G. S. (2004) Opportunistic amoebae: challenges in prophylaxis and treatment. *Drug Resistance Updates*, ***7*(1)**, 41–51.

3. De Moraes, J. and Alfieri, S. C. (2008) Growth, encystment and survival of Acanthamoeba castellanii grazing on different bacteria. *FEMS Microbiology Ecology*, **66(2)**, 221–229.

4. Polat, Z. A., Vural, A., Ozan, F., Tepe, B., Özcelik, S. and Cetin, A. (2008) In vitro evaluation of the amoebicidal activity of garlic (Allium sativum) extract on Acanthamoeba castellanii and its cytotoxic potential on corneal cells. *Journal of Ocular Pharmacology and Therapeutics*, **24(1)**, 8–14.

5. Visvesvara, G. S., Moura, H. and Schuster, F. L. (2007) Pathogenic and opportunistic free-living amoebae: Acanthamoeba spp., Balamuthia mandrillaris, Naegleria fowleri, and Sappinia diploidea. *FEMS Immunology & Medical Microbiology*, **50(1)**, 1–26.

6. Seal, D. V. (2003) Acanthamoeba keratitis update—incidence, molecular epidemiology and new drugs for treatment. *Eye*, ***17*(8)**, 893.

7. Siddiqui, R., Aqeel, Y. and Khan, N. A. (2016) The development of drugs against Acanthamoeba infections. *Antimicrobial Agents and Chemotherapy*, **60(11)**, 6441–6450.

8. Siddiqui, R. and Khan, N. A. (2012) Biology and pathogenesis of Acanthamoeba. *Parasites & Vectors*, **5(1)**,

9. Lorenzo-Morales, J., Martín-Navarro, C. M., López-Arencibia, A., Arnalich-Montiel, F., Piñero, J. E. and Valladares, B. (2013) Acanthamoeba keratitis: an emerging disease gathering importance worldwide? *Trends in Parasitology*, **29(4)**, 181–187.

10. Marciano-Cabral, F. and Cabral, G. (2003) Acanthamoeba spp. as agents of disease in humans. *Clinical Microbiology Reviews*, **16(2)**, 273–307.

11. Cannas, S., Usai, D., Tardugno, R., Benvenuti, S., Pellati, F., Zanetti, S. and Molicotti P. (2016) Chemical composition, cytotoxicity, antimicrobial and antifungal activity of several essential oils. *Natural Product Research*, **30(3)**, 332–339.

12. Singh, H. & Pathak, A (2018) *Review on Estimation of Eugenol in Herbal Plants. World Wide Journal of Multidisciplinary Research and Development*, **4(1)**, 344–347.

13. Carrasco, A., Espinoza, C., Cardile, V., Gallardo, C., Cardona, W., Lombardo, L., Catalán, M., Cuellar, F. & Russo, A. (2008) Eugenol and its synthetic analogues inhibit cell growth of human cancer cells (Part I). *Journal of the Brazilian Chemical Society*, **19(3)**, 543–548.

14. Bar, F. M. A., Khanfar, M. A., Elnagar, A. Y., Badria, F. A., Zaghloul, A. M., Ahmad, K. F., Sylvester, P. W. & El Sayed, K. A. (2010) Design and pharmacophore modeling of biaryl methyl eugenol analogs as breast cancer invasion inhibitors. *Bioorganic & medicinal chemistry*, **18(2)**, 496–507.

15. Awasthi, P. K., Dixit, S. C., Dixit, N. & Sinha, A. K. (2008) Eugenol derivatives as future potential drugs. *J Pharm Res*, **1(2)**, 216.

16. Leem, H. H., Kim, E. O., Seo, M. J. & Choi, S. W. (2011) Antioxidant and anti-inflammatory activities of eugenol and its derivatives from clove (Eugenia caryophyllata Thunb.). *Journal of the Korean Society of Food Science and Nutrition*, **40(10)**, 1361–1370.

17. Anacarso, I., Sabia, C., de Niederhäusern, S., Iseppi, R., Condò, C., Bondi, M. and Messi, P. (2017) In vitro evaluation of the amoebicidal activity of rosemary (Rosmarinus officinalis L.) and cloves (Syzygium aromaticum L. Merr. & Perry) essential oils against Acanthamoeba polyphaga trophozoites. *Natural Product Research*, **33(4)**, 606–611.

18. Rahim, N. H. C. A., Asari, A., Ismail, N. & Osman, H. (2017) Synthesis and antibacterial study of eugenol derivatives. *Asian Journal of Chemistry*, **29(1)**, 22.

19. Wright, C. W., O'neill, M. J., Phillipson, J. D. and Warhurst, D. C. (1988) Use of microdilution to assess in vitro antiamoebic activities of Brucea javanica fruits, Simarouba amara stem, and a number of quassinoids. *Antimicrobial Agents and Chemotherapy*, **32(11)**, 1725–1729.

20. Raja, M. R. C., Velappan, A. B., Chellappan, D., Debnath, J. & Mahapatra, S. K. (2017) Eugenol derived immunomodulatory molecules against visceral leishmaniasis. *European journal of medicinal chemistry*, **139**, 503–518.

21. d'Avila Farias, M., Oliveira, P. S., Dutra, F. S., Fernandes, T. J., de Pereira, C. M., de Oliveira, S. Q., Stefanello, F. M., Lencina, C. L. and Barschak, A. G. (2014) Eugenol derivatives as potential anti-oxidants: is phenolic hydroxyl necessary to obtain an effect? *Journal of Pharmacy and Pharmacology*, **66(5)**, 733–746.

22. Ito, M., Murakami, K. and Yoshino, M. (2005) Antioxidant action of eugenol compounds: role of metal ion in the inhibition of lipid peroxidation. *Food and Chemical Toxicology*, **43(3)**, 461–466.

23. Lam, K. S. (2007) New aspects of natural products in drug discovery. *Trends in Microbiology*, **15(6)**, 279–289.

24. Bhutani, K. K., Sharma, G. L. and Ali, M. (1987) Plant based antiamoebic drugs; Part I. Antiamoebic activity of phenanthroindolizidine alkaloids; common structural determinants of activity with emetine. *Planta Medica*, **53(06)**, 532–536.

25. Boyom, F. F., Ngouana, V., Zollo, P. H. A., Menut, C., Bessiere, J. M., Gut, J. and Rosenthal, P. J. (2003) Composition and anti-plasmodial activities of essential oils from some Cameroonian medicinal plants. *Phytochemistry*, **64(7)**, 1269–1275.

26. Walochnik, J., Duchêne, M., Seifert, K., Obwaller, A., Hottkowitz, T., Wiedermann, G. and Aspöck, H. (2002) Cytotoxic activities of alkylphosphocholines against clinical isolates of Acanthamoeba spp. *Antimicrobial Agents and Chemotherapy*, **46(3)**, 695–701.

27. Khairul, W. M., Goh, Y. P., Daud, A. I. and Nakisah, M. A. (2017) Cytotoxicity effects of alkoxy substituted thiourea derivatives towards Acanthamoeba sp. *Arabian Journal of Chemistry*, **10(4)**, 532–538.

28. Gessler, M. C., Nkunya, M. H., Mwasumbi, L. B., Heinrich, M. and Tanner, M. (1994) Screening Tanzanian medicinal plants for antimalarial activity. *Acta Tropica*, **56(1)**, 65–77.

29. Abid, M. and Azam, A. (2006) Synthesis, characterization and antiamoebic activity of 1-(thiazolo [4, 5-b] quinoxaline-2-yl)-3-phenyl-2-pyrazoline derivatives. *Bioorganic & Medicinal Chemistry Letters*, **16(10)**, 2812–2816.

30. Duggal, S. D., Rongpharpi, S. R., Duggal, A. K., Kumar, A. and Biswal, I. (2017) Role of Acanthamoeba in granulomatous encephalitis: a review. *J Infect Dis Immune Ther 1*, **1**, 2.

31. Elmore, S. (2007) Apoptosis: a review of programmed cell death. *Toxicologic Pathology*, **35(4)**, 495–516.

32. Lloyd, D. (2014) Encystment in Acanthamoeba castellanii: a review. *Experimental Parasitology*, **145**, S20–S27.

33. Riss, T., Niles, A., Moravec, R., Karassina, N. and Vidugiriene, J. (2019) Cytotoxicity Assays: In Vitro Methods to Measure Dead Cells. In *Assay Guidance Manual [Internet]*. Eli Lilly & Company and the National Center for Advancing Translational Sciences.

34. Emerson, J. B., Adams, R. I., Román, C. M. B., Brooks, B., Coil, D. A., Dahlhausen, K.Ganz, H.H., Hartman, E. M., Hsu, T., Justice, N. B. and Paulino-Lima, I. G. (2017) Schrödinger's microbes: tools for distinguishing the living from the dead in microbial ecosystems. *Microbiome*, *5***(1)**, 86.

35. Bank, H. L. (1988) Rapid assessment of islet viability with acridine orange and propidium iodide. *In vitro cellular & developmental biology*, **24(4)**, 266–273.

36. Lovecka, P., Thimova, M., Grznarova, P., Lipov, J., Knejzlik, Z., Stiborova, H., Nindia, T. J. D., Demnerova, K. and Ruml, T. (2015) Study of cytotoxic effects of benzonitrile pesticides. *BioMed Research International*, **2015**.

37. Chan, L. L. Y., Kuksin, D., Laverty, D. J., Saldi, S. and Qiu, J. (2015) Morphological observation and analysis using automated image cytometry for the comparison of trypan blue and fluorescence-based viability detection method. *Cytotechnology*, **67(3)**, 461–473.

38. Puranam, K. L. and Boustany, R. M. (1998) *Assessment of Cell Viability and Histochemical Methods in Apoptosis*, 129–152.

39. Wallen, C. A., Higashikubo, R. and Dethlefsen, L. A. (1982) Comparison of two flow cytometric assays for cellular RNA—acridine orange and propidium iodide. *Cytometry: The Journal of the International Society for Analytical Cytology*, **3(3)**, 155–160.

40. Cummings, B. S., Wills, L. P. and Schnellmann, R. G. (2004) Measurement of cell death in mammalian cells. *Current Protocols in Pharmacology*, **56(1)**, 12.8.1-12.8.24.

41. Cutler, S., Tworkoski, T. & Cutler, H. (2002) The Synthesis and Biological Evaluation of Eugenol Derivatives as Potential Herbicidal Agents. In *Plant Growth Regulator Society of America Meeting*, **29**, 93–98.